

CHAPTER II

EXPERIMENTAL DETERMINATION OF THE CURVATURE INDUCED REDUCTION IN THE SMECTIC A - NEMATIC TRANSITION POINT

2.1 Introduction

As already mentioned in chapter I, the smectic A phase is characterized by a two component order parameter¹ $\psi = |\psi| e^{i\phi}$, where ϕ , the phase of the order parameter, defines the position of the layers and $|\psi|$, the amplitude of the order parameter, describes the degree of smectic order. $|\psi|$ lies between 0 and 1. At $|\psi| = 0$, no layers exist. ψ is analogous to the order parameter of a superfluid. Further, because of the layered arrangement, smectic A does not allow a $|\text{curl } \vec{n}|$ type of distortion which requires a change of layer spacing and hence a rather large energy, indeed larger by many orders of magnitude than the curvature distortion in the nematic phase. Thus a $|\text{curl } \vec{n}|$ type of distortion is suppressed in the A phase. This is analogous to the Meissner effect in a superconductor, $|\text{curl } \vec{n}|$ being the analog of the magnetic field.

The close analogy between a second order A-N transition under $|\text{curl } \vec{n}|$ distortion and the superconductor-normal metal transition under a magnetic field was recognized by de Gennes¹ who constructed a Landau-Ginzburg free energy to describe the smectic A-nematic transition close to the transition point.

The free energy density is written as

$$\begin{aligned}
 F_S = F_0 + A|\psi|^2 + \frac{1}{2}B|\psi|^4 + \frac{1}{2M_V}|\partial_z\psi|^2 \\
 + \frac{1}{2M_t} \left\{ |(\partial_x + iq_0 n_x)\psi|^2 \right. \\
 \left. + |(\partial_y + iq_0 n_y)\psi|^2 \right\} + \phi_N \quad (2.1)
 \end{aligned}$$

where $\phi_N = \frac{1}{2} \left[k_{11}(\nabla \cdot \vec{n})^2 + k_{22}(\vec{n} \cdot \nabla \times \vec{n})^2 + k_{33}(\vec{n} \times \nabla \times \vec{n})^2 \right]$ is the nematic free energy, $A = A_0(T - T_c)$ and B which is a small positive quantity are the parameters of the Landau expansion, M_V and M_t are the components of the mass tensor along and perpendicular to the unperturbed director \vec{n}_0 (which lies along the z axis). M_V is inversely proportional to the elastic constant involved in the layer dilation and M_t is inversely proportional to the elastic constant of the director deformation relative to the layer normal, k_{11} , k_{22} and k_{33} are the Frank elastic constants and $\partial_z = \partial/\partial z$, etc.

In the A phase, the amplitude $|\psi|$ can be assumed to be constant and the gradient terms describe the gradients of the phase ϕ . The second gradient term describes the relative rotation of the layer normal with respect to the director. This relative tilt is significant only within a penetration depth λ given by

$$\lambda = \sqrt{\frac{2\epsilon_0 k_{ii} D}{q_0^2 A}}, \quad ii = 2 \text{ or } 3.$$

But deep inside the sample this deformation is absent and consequently $|\text{curl } \vec{n}|$ will not exist. The coupling between the director and the fluctuation of the smectic A order parameter above T_{AN} causes the divergence of the curvature elastic constants k_{22} and k_{33} as T is decreased to T_{AN} (de Gennes).¹ This is analogous to the divergence of the diamagnetic susceptibility in the normal phase as the superconducting transition is approached. (The three types of elastic deformations are illustrated in the previous chapter, fig. 1.4.) This prediction has been the subject of a large number of quantitative experimental investigations.²

Further, using the analogy with the superconductor-normal metal transition, de Gennes also predicted that T_{AN} , the smectic A - nematic transition temperature, should

be reduced if a twist or a bend distortion is imposed, just as a magnetic field reduces the superconductor-normal metal transition temperature. The detailed nature of the phase diagram of $|\text{curl } \vec{n}|$ against T_{AN} depends on the parameter $\kappa = \lambda/\xi$, where λ is the penetration depth of $|\text{curl } \vec{n}|$ type of distortion into the medium, and ξ the coherence length over which any perturbation influences the smectic order. If $\kappa < \frac{1}{\sqrt{2}}$ (type I materials), $|\text{curl } \vec{n}|$ distortion leads to reduction of T_{AN} and the transition becomes first order in character. Most smectics appear to be of type I character. However, if $\kappa > \frac{1}{\sqrt{2}}$, we have two critical distortions (type II materials). At the first critical distortion, A phase goes over to a mixed phase or Shubnikov phase. Under the second critical distortion, Shubnikov phase goes over to the classical nematic. Both these transitions are second order in character.

To estimate the effect of $|\text{curl } \vec{n}|$ in type I materials, we retain only the following terms in the free energy density for infinitely large samples.

$$F_s = F_0 + A|\gamma|^2 + \frac{B}{2}|\gamma|^4 + \frac{1}{2}k_{11} (\text{curl } \vec{n})^2$$

$i = 2$ for twist
 $i = 3$ for bend.

The minimisation of free energy of a deformation free sample yields the usual equation for the order parameter for $T < T_{AN}$

$$|\psi|^2 = -A/B \quad (2.2)$$

$$\text{with } A = A_0 (T - T_{AN}).$$

Hence, for the transition of the nematic with the $|\text{curl } \vec{n}|$ type of distortion

$$F_s = F_0 - \frac{A^2}{2B} + \frac{k_{11}}{2} (\text{curl } \vec{n})^2.$$

The N-A transition in this case obviously occurs when

$$A^2/B = k_{11} (\text{curl } \vec{n})^2 \quad (2.3)$$

which gives the threshold curve. The transition temperature is lowered to T_{AN}^d given by the relation

$$A = A_0 (T_{AN}^d - T_{AN}^0)$$

where T_{AN}^0 is the transition temperature of a deformation free sample. For $T_{AN}^d < T < T_{AN}^0$, the energy $\frac{1}{2}k_{11}(\text{curl } \vec{n})^2$ released on expelling the $(\text{curl } \vec{n})$ distortion is more than the energy gained, viz., $-A^2/2B$, by the medium from a transition to the A phase. At T_{AN}^d the two energies balance and the medium goes over to the A phase. Further, at this temperature, the order parameter $|\psi|$ is not zero, but has a finite value given by relation (2.2), and hence the transition takes first order characteristics.

There have been very few experimental studies

regarding this prediction. To our knowledge, there have been only two experiments in which this theoretical prediction has been taken into account to explain observations. Pa the first one by Cladis and Torza,³ a striped texture was observed when N-p-cyanobenzylidene-p'-octyloxyaniline (CBOOA) with a strong bend distortion was cooled to T_{AN} , and was interpreted in terms of the intermediate state. More recently, similar observations have been made by Rinov⁴ on a CBOOA sample with a bend deformation induced by an electric field. However, there has been no experimental determination of the phase diagram, i.e., the dependence of T_{AN} on $|\text{curl } \vec{n}|$. In this chapter we present the first experimental determination of such a phase diagram.

2.2 Experimental

Two experimental geometries have been used to determine the phase diagram.

(i) In the first, the deformation is induced by a magnetic field applied to a homogeneously aligned sample. The alignment was obtained by taking the sample between two glass plates whose inside surfaces were coated at an oblique angle with silicon monoxide. The thickness of the sample, measured using channelled

spectrum, was in the range of 20 to 50 μm . The sample was then mounted inside a heater provided with glass windows. The detailed construction of the heater is given in chapter IV. The heater was kept between the pole pieces of an electromagnet which could give a field strength up to 14 KGauss. The temperature of the sample was measured using a calibrated copper-constantan thermocouple and a Keithley 181 digital nanovoltmeter. In all our measurements, the temperature was measured to an accuracy of 0.01°C .

Schematic diagram of the experimental set up used to detect light scattered by bend fluctuations⁵ is shown in figure 2.1. Light from a 2 MW He-Ne laser was passed through a polarizer (P) and then through the sample at an oblique angle as shown in the diagram. The light scattered from the sample was passed through another polaroid (A) which lies in crossed configuration with respect to the polarizer P. The depolarized component of the scattered light with the scattering vector lying along the undistorted director was received by a photomultiplier (Model Hamamatsu type R585) whose output was fed to a photon counter (Spex digital photometer). The output from the photon counter and Keithley 181

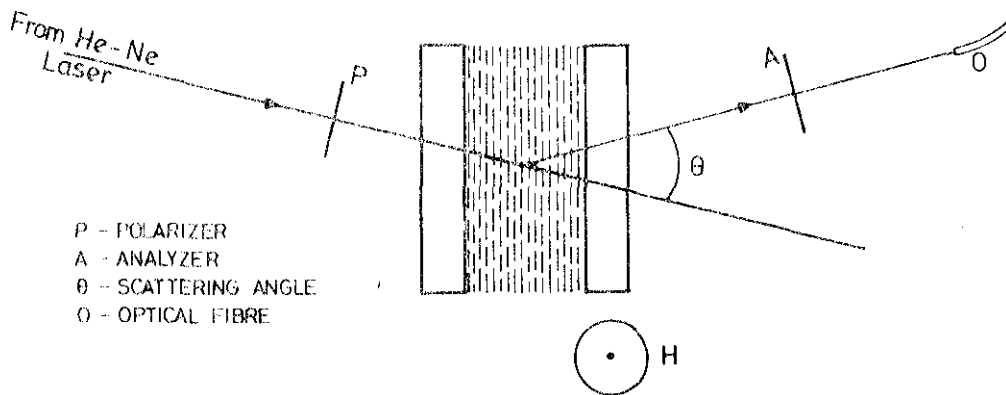


FIGURE 2.1

Schematic diagram of the experimental set up to detect light scattered by bend fluctuations, The magnetic field H applied perpendicular to the plane of the paper produces a twist distortion in the medium. For the sake of clarity, the thickness of the sample is very much exaggerated compared to that of the glass plate.

digital nanovoltmeter (used for temperature measurement) were connected to Y and X channels respectively of a Riken Denshi XY recorder. Thus the recorder plotted the intensity of scattered light against thermo e.m.f. Since the bend fluctuations are quenched in the A phase, the scattered light intensity increases as the sample is heated from the A phase to the N phase, and thus enables the detection of the AN transition point.

(ii) In the second method, two glass plates whose inside surfaces were coated with silicon monoxide at an oblique angle, are arranged in a twisted nematic configuration. The sample thickness was measured using the channelled spectrum technique to be described later. The cell was then filled with the liquid crystal and mounted inside a hot stage and the temperature of the sample was measured using a calibrated alumel-chromel thermocouple in conjunction with a Keithley 181 nanovoltmeter. The sample was observed through a polarizing microscope (Leitz Ortholux Model II POL-BK). Preliminary observations were made on cells with uniform thickness.

In order to determine γ as a function of $(\partial\phi/\partial x)$, we used a twisted nematic cell in the form of a wedge as shown in figure 2.2. The wedge angle was about 0.001

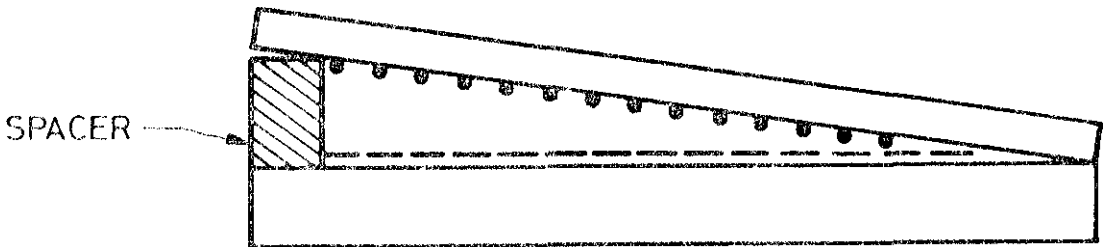


FIGURE 2.2

Schematic diagram of the wedge shaped twisted nematic cell used to determine the dependence of T_{AN} on $|\text{curl } \vec{n}|$. The dots and dashes represent the easy axes of alignment. In the actual experiment, the twist angle was $\simeq 75^\circ$.

radian. The thicknesses of the cell at various positions of the wedge in the section shown in fig.2.2 were determined by the channelled spectrum technique before the sample was filled. The actual twist angle at the desired point in the sample could be measured by noting the angles of the polarizer and the analyzer of the microscope for getting dark field of view when the sample was in the nematic phase. The angle could be measured to an accuracy of 1° .

The compounds studied are CBDA, 4-n-octyloxy-4'-cyanobiphenyl (8 OCB) and trans-4-propylcyclohexyl-4-(trans-4-pentylcyclohexyl)benzoate.

Thickness measurements

The thickness of the air film between two glass plates was measured using channelled spectrum. White light from a source S is rendered parallel by a convex lens L_1 and is made to fall normally on the air film enclosed between the glass plates (Fig.2.3). The light reflected from the two glass plates forming the air film is made to converge on the slit S_1 of a constant deviation spectroscop (Adair-Hilger Ltd.). Alternate bright and dark fringes are formed due to the interference of light

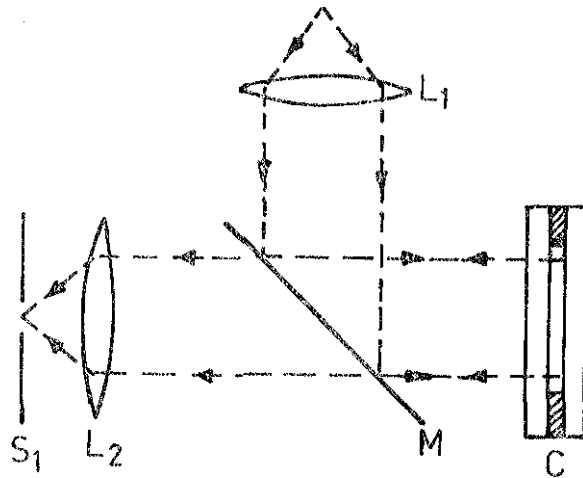


FIGURE 2.3

Arrangement to measure the thickness of the sample by forming the channelled spectrum.

reflected from the two surfaces forming the air film, The thickness of the air film can be calculated using the expression

$$x_0 = \frac{(n - m) \lambda_m \lambda_n}{2(\lambda_m \sim \lambda_n)}$$

where λ_m and λ_n are the wavelengths corresponding to the m^{th} and n^{th} dark fringes respectively.

2.3 Results and Discussion

(i) Twist deformation induced by a magnetic field.

If a homogeneously aligned nematic sample of thickness x_0 is subjected to a magnetic field (H) acting in the plane of the glass plates but perpendicular to the initial orientation of the director (\vec{n}) (fig. 2.1), for a field strength $H > H_c$ the Freedericksz threshold, the medium acquires a twist deformation $|\text{curl } \vec{A}| = d\phi(x)/dx$ with the X axis normal to the plates. The threshold field is given by

$$H_c = \frac{\pi}{x_0} \sqrt{\frac{k_{22}}{\Delta\chi}} \quad (2.4)$$

where $\Delta\chi$ is the anisotropy of the volume diamagnetic susceptibility of the medium.

$|\text{curl } \vec{n}|$ at any given point (x) for a field H ($> H_0$) is given by

$$\frac{d\phi(x)}{dx} = \frac{\pi}{x_0} \cdot \frac{H}{H_c} \left[\sin^2 \phi_m - \sin^2 \phi(x) \right]^{\frac{1}{2}} \quad (2.5)$$

where $\phi_m(H)$ is the maximum angle of twist at the midplane. $d\phi/dx$ takes the largest value near the boundaries and reduces to zero at the midplane. The maximum value is given by

$$\left(\frac{d\phi}{dx} \right)_{\text{max}} = \frac{\pi}{x_0} \cdot \frac{H}{H_c} \sin \phi_m(H) \quad (2.6)$$

The average value of $|\text{curl } \vec{n}|$ over the entire sample thickness is given by

$$\begin{aligned} \overline{\left(\frac{d\phi}{dx} \right)} &= \frac{\pi}{x_0} \cdot \frac{H}{H_c} \frac{\sin^2 \phi_m}{\phi_m} \left[\left(1 - \frac{1}{\sin^2 \phi_m} \right) \frac{\pi}{2} \cdot \frac{H}{H_c} \right. \\ &\quad \left. + \frac{1}{\sin^2 \phi_m} E(\sin \phi_m, \frac{\pi}{2}) \right] \quad (2.7) \end{aligned}$$

where $E(\sin \phi_m, \pi/2)$ is the complete elliptic integral of the second kind. For $H < 2.5 H_0$, $\overline{\left(\frac{d\phi}{dx} \right)} > \frac{2}{3} \left(\frac{d\phi}{dx} \right)_{\text{max}}$. As the magnetically deformed sample is cooled below T_{AN} , one expects that the A phase is formed at the midplane (where $\frac{d\phi}{dx} = 0$) and grows toward the boundaries

at lower temperatures. Our visual observation clearly showed the reduction of T_{AN} on application of a sufficiently strong field. If the sample is cooled under the field to a temperature slightly lower than T_{AN}^0 (the superscript 'o' standing for $H = 0$), and H is reduced to zero, the transition to the A phase occurred immediately. The N-A front could be moved by changing the value of H . Further, on careful observations it was noticed that the N-A transition under the field was really complete only when the temperature is lowered by a considerable value. For example, if $d \approx 25 \mu$, $H \approx 14,000$ Gauss, transition is complete only for $T \approx T_{AN}^0 - 2^\circ$. The large temperature range of the "intermediate state" is probably due to the continuous increase in the value of $|\text{curl } \vec{n}|$ as the growing smectic layer squeezes the nematic region into a progressively thinner region as the temperature is lowered. We could also observe the reduction in T_{AN} in the heating mode, under the action of H . The transition point was detected by the light scattering technique as explained in the experimental part.

The field dependences of T_{AN} for CBOOA (which has almost a second order A-N transition⁶) and B OCB (which has an extremely weak first order AN transition⁷) are

shown in figs. 2.4 and 2.5 respectively. Though we get the correct trend in both the cases, it is difficult to estimate the actual value of $|\text{curl } \vec{n}|$ for the following reasons: (a) $d\phi/dx$ is non-uniform across the sample, as discussed earlier, and (b) the value of H_c is difficult to estimate at T_{AN} (H_c is expected to tend to ∞ as $k_{22} \rightarrow \infty$ at T_{AN}). Hence this method is not suitable for determining the phase diagram quantitatively.

(ii) Studies on 'twisted nematic' cells

A nematic sample taken in a twisted cell has a uniform $|\text{curl } \vec{n}| = \frac{d\phi}{dx} = \frac{\phi_1 - \phi_2}{x_0}$, where $(\phi_1 - \phi_2)$ is the twist angle which is chosen to be about 75° in our experiments.

Observations on twisted nematic cells of uniform thickness x_0 showed that the transition to the A phase first started near the glass boundaries and could be recognized by the appearance of folds (fig. 2.6a).

However fluctuations in the intensity of light could also be seen indicating the coexistence of A and N phases. The "intermediate state" (fig. 2.6b) again lasted &—
 $\sim a \sim T_{AN} = PC_1$ for reasons already mentioned. When entire sample was transformed to the A phase (fig. 2.6c),

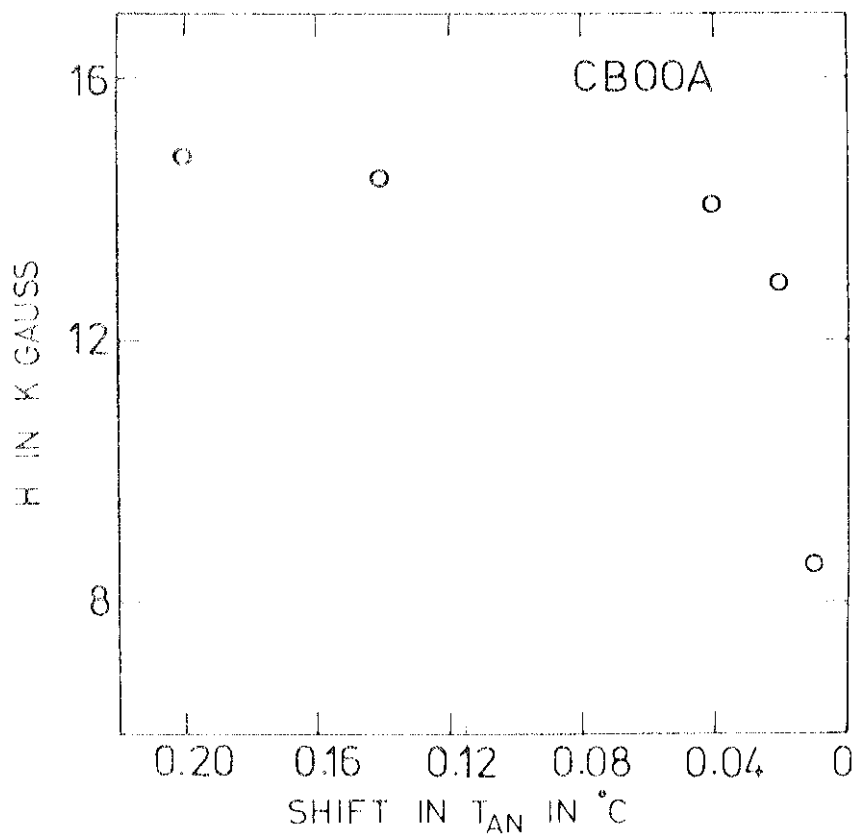


FIGURE 2.4

Magnetic field dependence of the shift in T_{AN} for a 25 μm thick sample of CBOOA

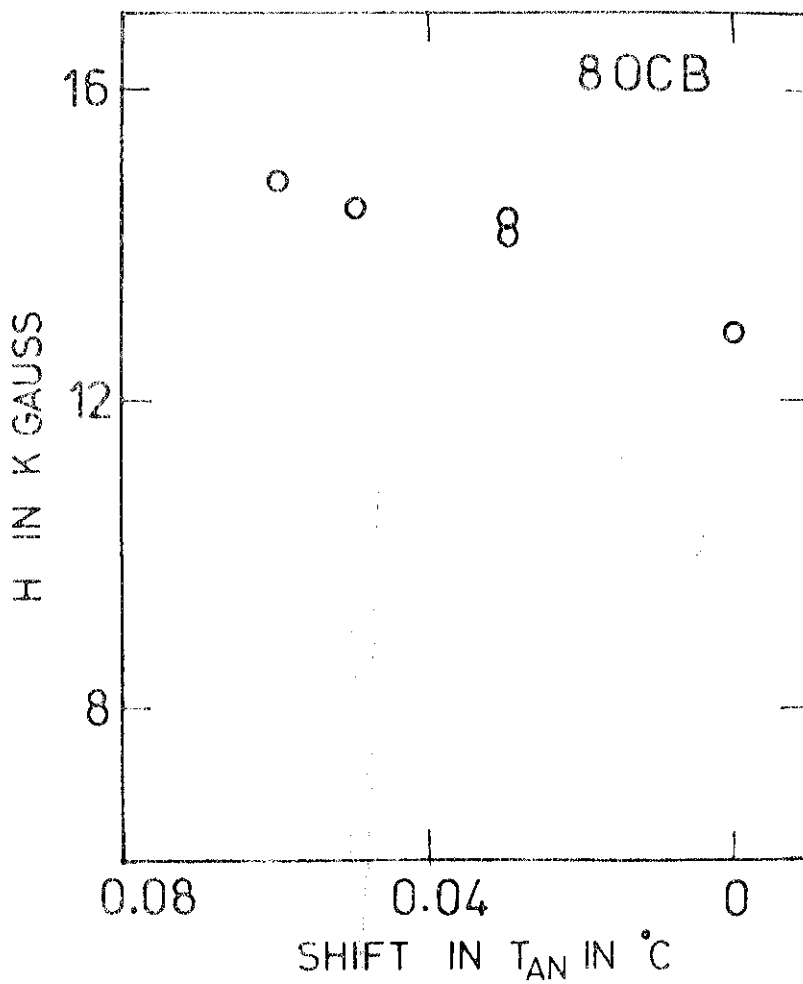
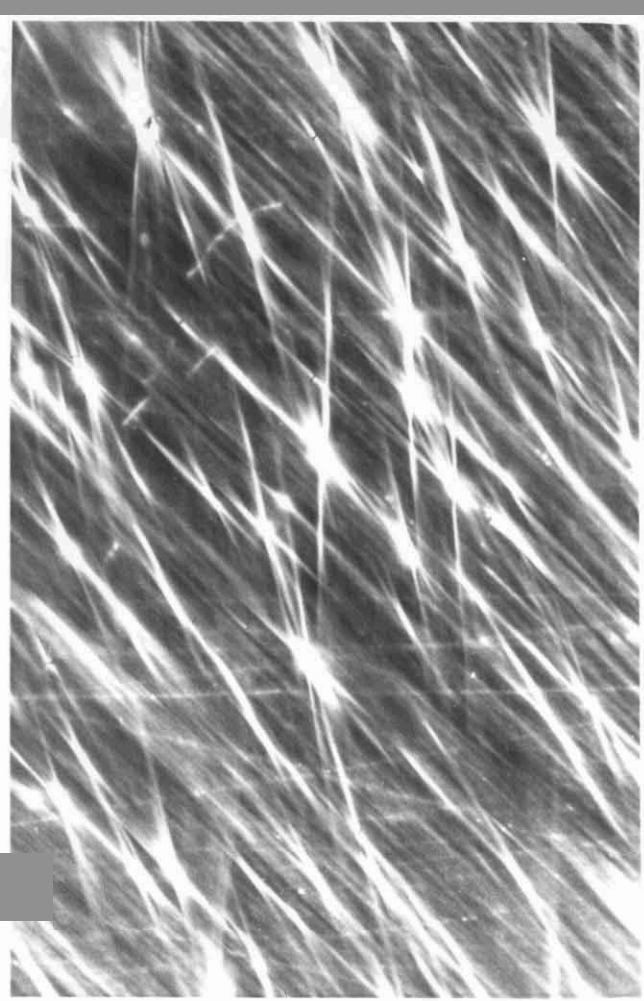
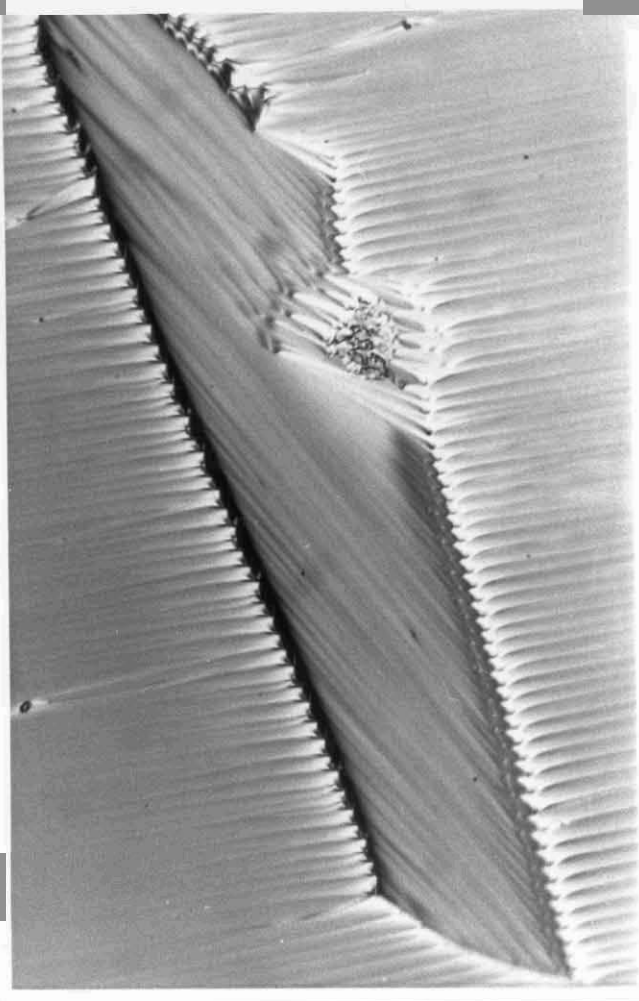


FIGURE 2.5

Magnetic field dependence of the shift in T_{AN} for a 25 μm thick sample of 8 OCB.



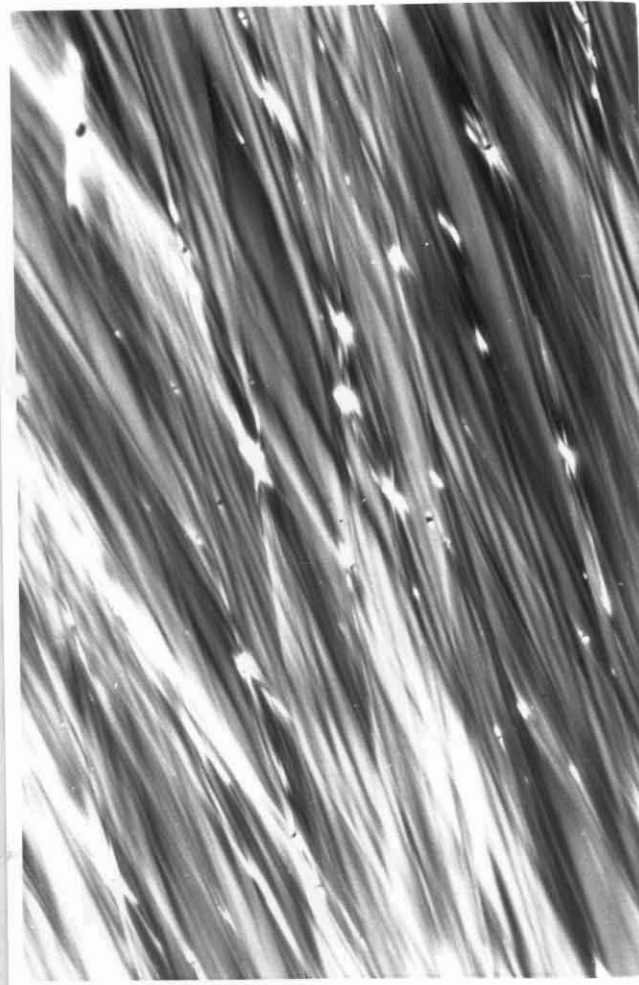
(a)



(d)



(c)



(b)

FIGURE 2.6

Photographs of various aspects of 'twisted nematic' samples of CBOOA cooled below T_{AN}^0 (polarizers adjusted to get a relatively dark field of view). (a) A sample of thickness $50\ \mu\text{m}$ at 82.7°C . Focussed on the bottom plate: Notice that the A phase has started to appear in the form of folds which are aligned along the diagonal from the top left corner to the bottom right corner, corresponding to the orientation of the molecules on the bottom plate (400 x). (By focusing the microscope on the top plate, similar folds aligned in a different direction corresponding to the orientation of the molecules on the top plate could be seen.) (b) Another sample (thickness = $15\ \mu\text{m}$) at 82.4°C focused on the midplane. The easy axes of the molecules on the top and bottom plates are nearly vertical and horizontal respectively. Folds and strong fluctuations of the director were seen simultaneously in the field of view, indicating the coexistence of A and N phases. (c) Same sample as in (b) but at 78.6°C . The entire sample is filled with folds of the A phase. No fluctuations are seen, indicating that the transition to the A phase is complete. Notice that the average alignment of the folds is $\sim 45^\circ$ to the vertical. (d) Nematic island seen in a $15\ \mu\text{m}$ thick sample.

the folds corresponded to an orientation midway between ϕ_1 and ϕ_2 . In thin samples, sometimes one could see small islands in which the general alignment was different from the surroundings, probably due to defective coating and/or non-uniformity of the glass surfaces (fig. 2.6d).

As pointed out earlier, a wedge shaped twisted nematic cell was used to determine T_{AN} as a function of $d\phi/dx$. By careful observation, the temperature at which the folds just appeared (as in fig.2.6a) at any given point was noted down. This temperature is taken to be the value of T_{AN}^t (the superscript 't' indicating a 'twisted' sample) corresponding to the initial value of $|\text{curl } \vec{n}|$ at that point. The results on CBOOA are shown in fig.2.7. Using a dimensional argument one can write equation (2.5) as³

$$T_{AN}^t = T_{AN}^0 - l T_{AN}^0 |\text{curl } \vec{n}| \quad (2.8)$$

where superscript 't' indicates the value for the twisted region and l is a molecular dimension. Equations (2.5) and (2.8) predict a linear variation of T_{AN}^t with $|\text{curl } \vec{n}|$ close to T_{AN}^0 .

Using the data near T_{AN}^0 , we find that $l \approx 45 \text{ \AA}$.

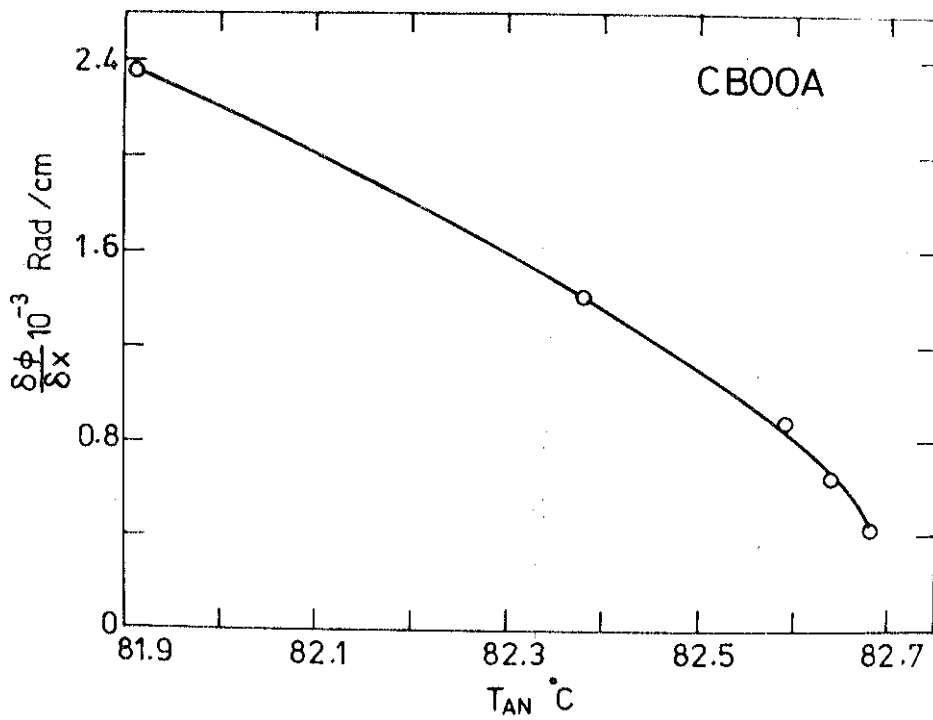


FIGURE 2.7

Variation of T_{AN} with $\frac{\delta\phi}{\delta x}$ for CBOOA.

For the twist deformation, λ should be compared to a transverse dimension of the molecules, and the large value that we obtain may mean that λ represents the dimension of a short range ordered group. The anti-parallel correlations between the strongly polar CBOOA molecules give rise to strong short ^{range} order effects even far above T_{AN} .

The results on B OCB are shown in fig.2.8. The reduction in T_{AN} is somewhat smaller than in the case of CBOOA for the same ϕ/α . Using the data close to T_{AN}^0 , $\lambda \simeq 15 \text{ \AA}$ which is also considerably shorter than that found for CBOOA though still larger than a molecular diameter. These results are in qualitative agreement with the trends shown by our experiments with the magnetic field induced distortions (figs. 2.4 and 2.5).

Both CBOOA and B OCB form partial bilayer smectics due to antiparallel interactions between neighbouring molecules with the strongly polar cyano end groups. We have carried out preliminary experiments on trans-4-propylcyclohexyl-4-(trans-4-pentyl cyclohexyl)benzoate which exhibits an almost second order AN transition at 55°C . This compound does not have a highly polar end group and is expected to exhibit a monolayer smectic.

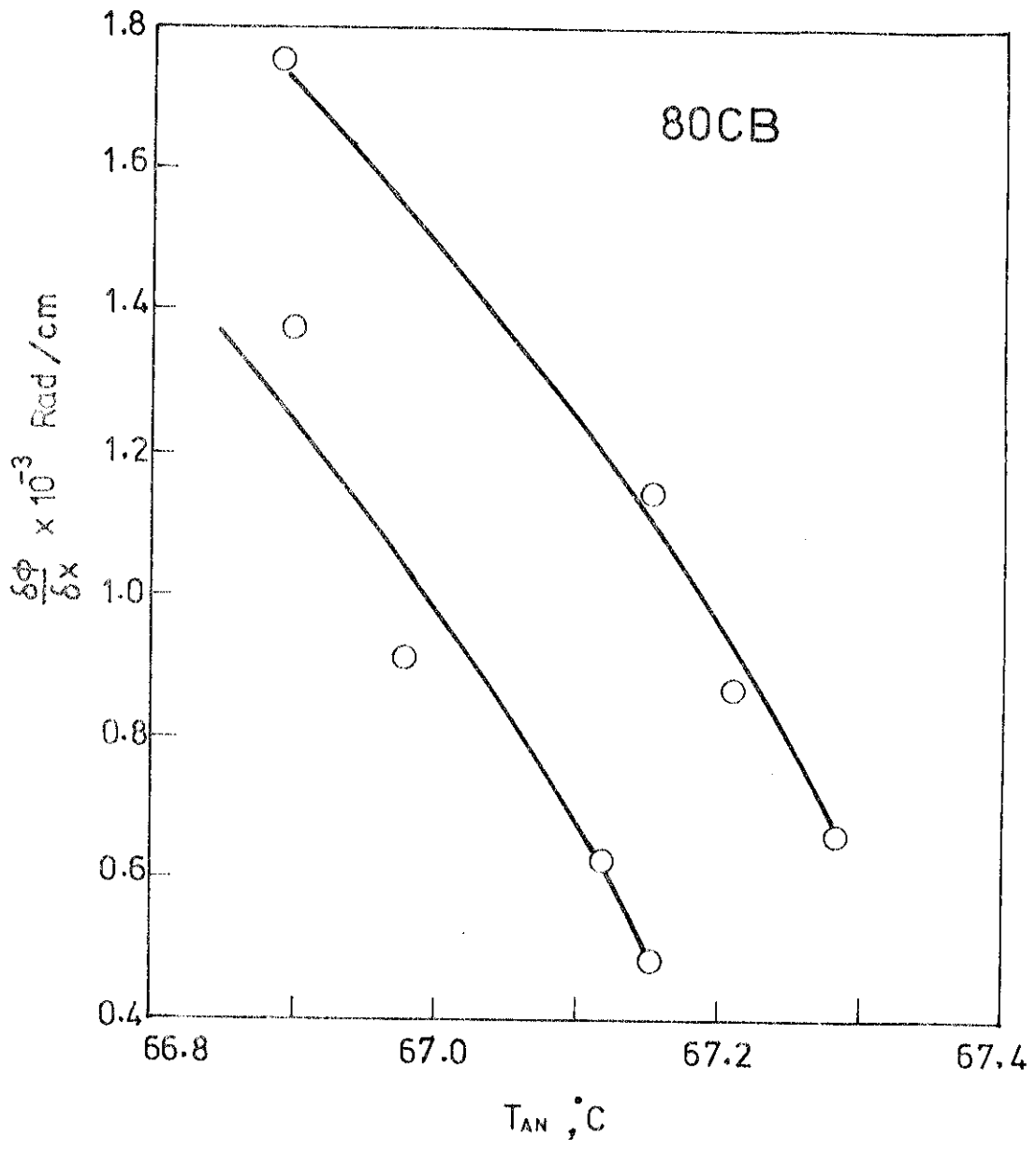


FIGURE 2.8

Variation of T_{AN} with $\delta\phi/\delta x$ for 8 OCB. Two curves represent two independent measurements with two different cells.

The results indicate a very weak reduction of T_{AN} , which is decreased by less than 0.1°C for $\partial\phi/\partial x \times 10^{-3} \simeq 1.8$. This indicates that the value of λ in this case is $\simeq 4.5 \text{ \AA}$ comparable to a molecular diameter.

REFERENCES

- 1 P.G. de Gennes, Solid State Commun. 10, 753 (1972);
Also P.G. de Gennes, Mol. Cryst. Liq. Cryst. 21, 49
(1973).
- 2 For a review, see S. Chandrasekhar and N.V. Madhusudana,
in Progress in Liquid Crystals, Ed. C.A. Croxton (John
Wiley and Sons, 1978), Chapter 14.
- 3 P.E. Cladis and S. Torza, J. Appl. Phys. 46, 994 (1975).
- 4 H.P. Ninov, J. de Physique, 42, 307 (1981).
- 5 H. Birecki and J.D. Litster, Mol. Cryst. Liq. Cryst.
42, 33 (1977).
- 6 K.C. Chu and W.L. McMillan, Phys. Rev. A11, 1099
(1975).
- 7 G.B. Hastings, K.J. Lushington and C.W. Garland,
Phys. Rev. 220, 321 (1980).